Cell Resolution 3D Reconstruction of Developing Multilayer Tissues from Sparsely Sampled Volumetric Microscopy Images

Anirban Chakraborty*, Ram Kishor Yadav†, G. Venugopala Reddy†, Amit K. Roy-Chowdhury*‡
*Department of Electrical Engineering, University of California, Riverside
†Department of Botany and Plant Sciences, University of California, Riverside
‡For Correspondence: amitrc@ee.ucr.edu

***Abstract*—Understanding of the growth dynamics in developmental biology is often pursued through the analysis of cell sizes and shapes obtained from CLSM based imaging at cell resolution of multi-layer tissues. This necessitates the development of robust 3D reconstruction methods using such images. However, all of the current methods of 3D reconstruction using CLSM imaging require large number of cell slices. But in the case of live cell imaging, i.e., imaging a growing tissue, such high depth resolution is not feasible in order to avoid photodynamic damage to the growing cells from prolonged exposure to laser radiation. In this work, we have addressed the problem of 3D reconstruction at cell resolution of a developing multi-layer tissue in the plant meristem when the amount of data is as limited as two to four slices per cell. This introduces significant image analysis challenges in terms of sparsity of the data, low signal-to-noise ratio, and a wide range of shapes and sizes. Motivated by the physical structure of the cells, we propose to reconstruct a cell cluster as a packing of truncated ellipsoids representing the individual cells. We test the proposed computational method on time-lapse CLSM images of Shoot Apical Meristem (SAM) cells of model plant Arabidopsis Thaliana. We show that the 3D reconstruction can lead to 3D shape models of complete cell clusters, which is an essential first step towards obtaining growth statistics for individual cells.**

I. Introduction

Proper understanding of the causal relationship between cell growth patterns and gene expression dynamics is one of the major topics of interest in developmental biology. Information such as rates and patterns of cell expansion play a critical role in explaining cell growth and deformation dynamics and thereby can be extremely useful in understanding morphogenesis. The need for quantifying these biological parameters (such as cell volume, cell growth rate, cell shape, mean time between cell divisions etc.) and observing their time evolution is of utmost importance to biologists. For complex multi layered, multi cellular plant and animal tissues, the only possible method to capture individual cell structures and to estimate the aforementioned parameters for growing cells is the Confocal Microscopy based *Live Cell Imaging*. Through this technique we can image tissues as a collection of serial optical slices which can then be used for analysis. However, in most cases, manual analysis (which has been the trend) is usually extremely tedious and, often, only provides qualitative trends in the data rather than precise quantitative models.

Of late, there has been a substantial amount of work in automated processing and analysis of cellular images - though mostly on image segmentation and cell tracking. Methods such as [1], [16] show that individual cells can be efficiently segmented in a multicellular field and [6], [10] provide automated methods to track individual cells in time. Estimation of cell shape and volumes as a function of time is most fundamental to understanding of the growth process. Due to the large quantity of data collected during the growth of a tissue, computational methods for robust estimation of 3D cell structures and cell volumes are absolutely necessary in order to obtain statistically significant results of these growth parameters.

There are some recent techniques [11] that investigated the problem of 3D reconstruction of cells in multi layered plant tissues using large number of image slices. But if dense samples in one time point are collected, it is highly unlikely that we will be able to get time lapse images as the specimen will not continue to grow in time due to high radiation exposure. Therefore the number of slices in which a cell is imaged is often very low (2-4 slices per cell). From an image analysis perspective, we are looking at a very challenging problem where we want to obtain a 3D surface reconstruction of arbitrary cell shapes from a set of very sparsely sampled data points in presence of unavoidable imaging noise. This motivates us to propose a novel 3D reconstruction based on physics based prior geometrical models for each cell in the tissue.

A. Relation to Existing Work

There are several methods of volume estimations for individual cells such as impedance method [12] and light microscopy methods [4]. Methods such as [7] are used to study changes in cell volumes in cell monolayers. But we are looking at a much more challenging problem where the subject of study is a dense cluster of cells. Plant meristem is one example of such cell clusters where hundreds of small cells are densely packed into a multilayer structure (Figure

This work is partially funded by National Science Foundation grants (IIS-0712253) to ARC and (IOS-0718046) to GVR.

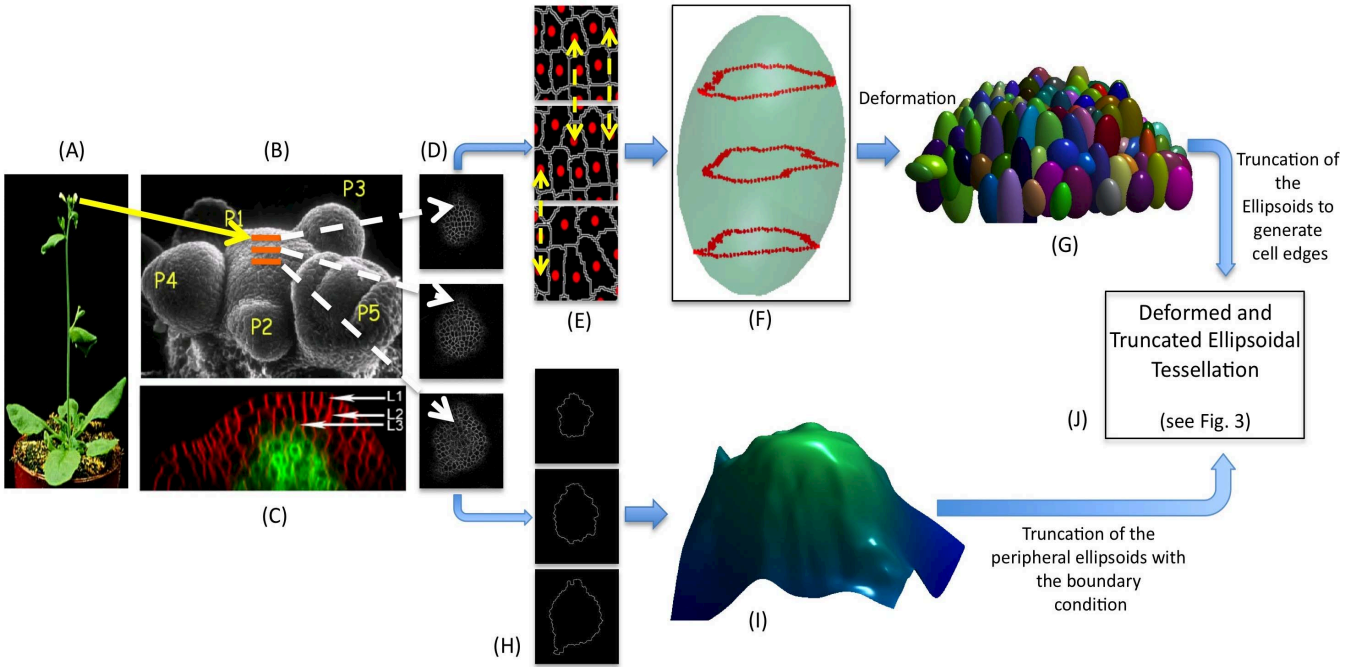

Figure 1. SAM cell cluster and the overview of the proposed cell volume estimation scheme. (A) SAM located at the top of the shoot of Arabidopsis, (B) A detailed surface view showing different regions of SAM, (C) A cross sectional side view of SAM, which clearly shows the multiple layers (L1, L2, L3) of tightly packed stem cells and their shapes, (D) Raw Images obtained through CLSM technique: Three consecutive optical slices of Arabidopsis Shoot Apical Meristem, (E) Preprocessed, segmented and tracked cell slices : A sample result showing the output of a Watershed segmentation and a tracking algorithm [10]. The arrow indicates a cell's correspondence in consecutive Z slices, (F) Contours of a single cell in three consecutive slices and the axis-aligned enclosing ellipsoidal approximation of the cell : The ellipsoid enclosing all the three cell contours (MVEE) (Sec. III-A), (G) The MVEEs estimated for each individual cell in a cluster are deformed (Sec. III-C) along their axes until the stopping criterion (Sec. III-C) is met. The deformed 3D ellipsoidal shapes of the cells in a dense cluster of around 200 cell are shown, (H) Segmented SAM contours using level-set method, (I) A smooth surface is fitted to the segmented SAM contours (Sec. III-B). The surface represents the global shape of the SAM, (J) The deformed ellipsoids for individual cells are truncated along the surface of intersections with their neighboring ellipsoids (Sec. III-D). The cells at the periphery of the SAM are also truncated by the estimated SAM surface. The truncated ellipsoids, densely packed together, represent the final 3D reconstruction of the SAM cell cluster (Fig. 3).

1(B, C, D)) and there is no experimental technique in the developmental biology framework which yields individual cell volumes in such a multi-layered cell structure. In such cases, the most popular practice is to use Confocal Laser Scanning Microscopy (CLSM) to image cell-slices at a very high spatial resolution and then reconstruct the 3-D volume of the cell from those serial optical slices [3], [5].

However, performance of the current image analysis methods on CLSM images depends heavily on the availability of a large number of very thin optical slices of a cell and the performance rapidly deteriorates in the cases where the number of cell slices becomes limited. Since one of the objectives for studying developing tissues is to understand the growth properties of individual cells, it is critical that each cell remains alive all throughout the imaging process. In order to keep the cells alive and growing for a longer period of time and obtain frequent observations, a cell can not be imaged in more than 2-4 slices, i.e., high depth-resolution and time-resolution cannot be achieved simultaneously. With such a limited amount of image data, the existing 3-D reconstruction techniques cannot yield a good estimate of individual cell volumes.

B. Contributions of the Proposed Method

In this paper, we focus on the Shoot Apical Meristem (SAM) of a developing plant. The Shoot Apical Meristem is a multilayer, multicellular structure where the cells are tightly packed together with hardly any void in between. Motivated by this knowledge of the physical structure of SAM, we propose a novel deformed truncated ellipsoidal model for each cell to obtain a cell resolution 3D reconstruction of the meristem from a very sparse Z-stack of confocal image slices. The multi-stage framework comprises of an initialization stage where the segmented individual plant cells are approximated by the Minimum Volume Enclosing Ellipsoids, followed by a deformation and a truncation stage. The global shape of the SAM is estimated to generate a boundary condition that limits the ellipsoids' deformation in the periphery of the SAM while the deformed and truncated ellipsoids represent the final 3D shape of individual cells. We present a mathematically rigorous framework to estimate the ellipsoids and perform the deformation given a sparse set of slices with the segmented cells in each slice. The process can deal with different kinds of segmentation errors in preprocessing of the noisy image data as long as proper Z-

correspondences among cell slices can be obtained through tracking.

II. Overview of the Proposed Method

A. Imaging Setup and Preprocessing

The SAM of *Arabidopsis Thaliana* consists of approximately 500 cells and they are organized into multiple cell layers that are clonally distinct from one another. By changing the depth of the focal plane, CLSM can provide in-focus images from various depths of the specimen. To make the cells visible under laser, fluorescent dyes are used. The set of images, thus obtained at each time point, constitute a 3-D stack, also known as the 'Z-stack'. Each Z-stack is imaged at a certain time interval (e.g. 3 hours between successive observations) and it is comprised of a series of optical cross sections of SAMs that are separated by approx. 1.5 μm (Fig. 1(B, D)). A standard shoot apical meristematic cell has a diameter of about 5 - 6 μm and hence in most cases, a single cell is not visible in more than 3-4 slices. To account for any minor shift in the alignment of the images in the 3-D stack, each stack is registered by a method of maximization of mutual information [14].

As we are interested in computing volume of every cell in the SAM cell cluster, we need to segment out all the cells in each slice. We can employ various segmentation algorithms like Watershed [13], Level-Set segmentation [1] etc. which have their own advantages and disadvantages. The method we propose here is independent of the segmentation strategy we choose to employ. In fact, the contribution of our method lies in the post segmentation and tracking stage.

In order to find a cell's correspondence across multiple slices in both the spatial and temporal direction, we have used our local-graph matching based robust cell tracking algorithm [10]. This algorithm starts by finding out a *seed cell pair* between two SAM slice images using 'local graph matching' and progressively moves outward from the seed-pair to obtain correspondences between neighboring cells until all the cells are tracked. This method is robust because it fuses tracking results over the entire 4-D image stack and thereby minimizes the chances of losing a cell in any of the slices caused by poor segmentation of noisy data.

B. Proposed 3D Reconstruction - Overview

Once we have the segmented contours of each of the cells in consecutive slices, the objective is to obtain 3D reconstruction of these cells. As explained above, the number of slices in which a particular cell can be present is very small (e.g. 2-4 slices/cell). Unfortunately, the existing 3-D reconstruction methods are not capable of handling such sparsity in data. Motivated by the physical structures of the cells, we handle this issue by assuming a prior 3D model for each cell shape which can then be deformed to fit the given sparse set of segmented cross sectional images. This makes the problem of 3-D reconstruction and cell volume estimation tractable. In this work, the prior model assumed for each cell is an ellipsoid.

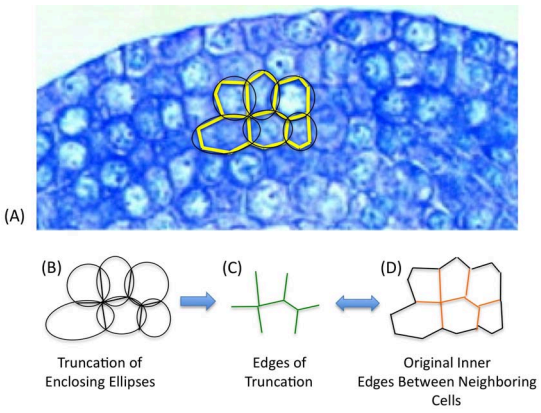

Figure 2. Cells As Truncated Ellipsoids - Motivation. (A) A cross sectional side view of SAM [15], where the cell walls are marked yellow and enclosing ellipses for each cell cross section is estimated, (B, C, D) The intersecting edges of the overlapping enclosing ellipses (MVEE) for neighboring cells replicate the original inner cell walls.

There can be several different ellipsoidal approximations for the segmented cells such as Minimum Volume Enclosing Ellipsoids (MVEE), Maximum Volume Inscribed Ellipsoids (MVIE), Least-Square Ellipsoids etc. Depending on the quality of the segmentation output, one approximation is preferred over the other. In plant cell clusters like SAM, cells are closely packed together and there is hardly any void between two neighboring cells. In such situations, the enclosing ellipsoidal (MVEE) approximations for individual cells overlap (Fig. 2(A)). The truncated enclosing ellipsoids (truncated along its intersections with the neighboring ellipsoids) are the closest representations of individual cell shapes (Fig. 2(B, C, D)). Motivated by this observational fact, we propose a novel 3-D reconstruction technique which computes the 3D shape of a cell not only from its own slice information, but also from information of the neighboring cells. Especially, in situations with poor imaging and large segmentation errors the cell shape estimates would be more accurate if we incorporate the neighborhood structural information into our estimation strategy. Because of the sparsity of the image data, the ellipsoids estimated for cell slice contours are not guaranteed to optimally overlap with their neighbors. The deformation stage (Section III-C) ensures that each of the 3D points inside the SAM structure is a part of a cell, thereby preserving the tightly packed physical structures of the SAM cells.

The proposed algorithm consists of four stages which are described as follows.

1. We estimate MVEE for each cell (Fig. 1(F)). We represent each cell by this ellipsoidal approximation and align the ellipsoids along the vertical axis of alignment of the segmented cell slices (Sec. III-A).

2. The global structure of the SAM is estimated by fitting a

smooth surface on the segmented SAM contours (Sec. III-B). The estimated 3D structure (Fig. 1(I)) is sampled to generate a dense 3D point cloud which is utilized in evaluating the stopping criterion of the ellipsoid deformation stage. The sampled points on 3D SAM surface also serve as boundary points for the peripheral cells in the truncation stage.

3. The MVEEs for the neighboring cells either do not overlap or non-optimally overlap (especially, along the Z axis of the 3D SAM stack due to the sparsity in the Z sampling). To deal with such cases, we deform the ellipsoids for each of the cells along their axes until a stopping criterion is satisfied. At this stopping point, each of the 3D points in the dense point cloud (computed in step 3) in SAM is inside atleast one of the deformed ellipsoids (Fig. 1(G), Sec. III-C).

4. In the final stage, we truncate the deformed ellipsoids along their plane(s) of intersection with the neighboring ellipsoids. The deformed ellipsoids for the peripheral cells are also truncated at the boundary of the SAM (Sec. III-D). The resultant truncated ellipsoidal structures represent the final 3D cell shapes.

In the next Section, we present each of these stages in details.

III. Detailed 3D Reconstruction Framework

A. Minimum Volume Enclosing Ellipsoid

After registration, segmentation and identification of a cell in multiple slices in the 3-D stack, we can obtain (X, Y, Z) co-ordinates of the set of points on the perimeter of the segmented cell slices. Let this set of points be $\mathcal{P} = \{p_1, p_2, \cdots p_n\} \in \mathbb{R}^3$. We have to estimate the minimum volume ellipsoid which encloses all these n points in $\mathbb{R}^3$ and we denote that with MVEE($\mathcal{P}$). An ellipsoid in its center form is represented by

$$\mathcal{E}(c, \Sigma) = \{p \in \mathbb{R}^3 \mid (p-c)^T \Sigma (p-c) \leq 1\} \quad (1)$$

where $c \in \mathbb{R}^3$ is the center of the ellipsoid $\mathcal{E}$ and $\Sigma \in \mathbb{R}^{3\times 3}$. Since all the points in $\mathcal{P}$ must reside inside $\mathcal{E}$, we have

$$(p_i - c)^T \Sigma (p_i - c) \leq 1 \text{ for } i = 1, 2, \cdots n \quad (2)$$

and the volume of this ellipsoid is

$$Vol(\mathcal{E}) = \frac{4}{3}\pi \{det(\Sigma)\}^{-\frac{1}{2}} \quad (3)$$

Therefore, the problem of finding the Minimum Volume Enclosing Ellipsoid (MVEE) for the set of points $\mathcal{P}$ can be posed as

$$\begin{aligned} \min_{\Sigma, c} \quad & - log\ det(\Sigma) \\ \text{s.t.} \quad & (p_i - c)^T \Sigma (p_i - c) \leq 1 \quad \text{for } i = 1, 2, \cdots n \\ & \Sigma \succ 0 \end{aligned} \quad (4)$$

To efficiently solve Problem (4) we convert the primal problem into its dual problem since the dual is easier to solve. A detailed analysis on the problem formulation and its solution can be found in [8], [9]. Once the ellipsoids are estimated, we align these ellipsoids along the estimated cell axis[1].

B. Estimation of Global Shape of The SAM

At this stage, we estimate the 3D structure of the SAM by fitting a smooth surface to its segmented contours. The surface fitting is done in two steps. In step one, the SAM boundary in every image slice is extracted using the 'Level Set' method (Fig. 1(H)). A level set is a collection of points over which a function takes on a constant value. We initialize a level set at the boundary of the image slice for each SAM cross section, which behaves like an active contour and gradually shrinks towards the boundary of the SAM. Let the set of points on the segmented SAM contours be P^{SAM} ($\{x^{SAM}, y^{SAM}, z^{SAM}\}$).

In the second step, we fit a surface on the segmented points P^{SAM}. Assuming that the surface can be represented in the form $z = f(x, y)$ (where the function f is unknown), our objective is to predict z at every point (x, y) on a densely sampled rectangular grid of points bounded by $\left[x^{SAM}_{min}, y^{SAM}_{min}, x^{SAM}_{max}, y^{SAM}_{max}\right]$. As the segmented set of data points are extremely sparse, this prediction is done using a linear interpolation on a local set of points on the grid around the point (x, y). As the value (z) for the point (x, y) is approximated by a linear combination of the values at a few neighboring points on the grid, the interpolation problem can be posed as a linear least-square estimation problem. We also impose a smoothness constraint in this estimation by forcing the first partial derivatives of the surface evaluated at neighboring points to be as close as possible. A MATLAB visualization [2] of the surface is shown in Fig. 1(I).

Once the SAM surface (S^{SAM}) is constructed, we uniformly sample a dense set of 3D points (P^D) such that every point in P^D must lie inside S^{SAM}. This dense point cloud is utilized in defining the stopping criterion of the ellipsoid deformation stage, as described in the next section.

C. Deformation of The Ellipsoids

After the initial MVEE estimation stage, the ellipsoids may not overlap or non-optimally overlap with their neighboring ellipsoids. This means the volume of the void space between the cells can be decreased if we deform all the ellipsoids along their axes. To deform an ellipsoid we first perform an eigen decomposition on the matrix Σ (Equation (1)) to obtain the eigen vectors and eigen values as,

$$\Sigma = VDV^{-1} \quad (5)$$

where V is the 3×3 eigen vector matrix and D is a 3×3 diagonal matrix comprised of the eigen values $(\lambda_1, \lambda_2, \lambda_3)$ of Σ as its diagonal entries. Now, the equatorial radii of the ellipsoid are $r_i = 1/\sqrt{\lambda_i},\ i = 1, 2, 3$. Therefore, a

[1]Please refer to the supplementary material at http://www.ee.ucr.edu/ amitrc/publications.php for details.

deformation $r_i^{'} = fr_i$ can be alternatively expressed as $\lambda_i^{'} = \lambda_i / f^2$ and the matrix Σ for the deformed ellipsoid can be recomputed using Equation(5).

In our method, we implement the deformation process in an iterative fashion. At each step of the iteration, we deform all the axis-aligned ellipsoids by the same factor f (> 1) along their axes. Then we check whether every point in P^D lies within at least one of the ellipsoids. We continue the deformation as long as the stopping criterion is not met, i.e. there exists a point in P^D which is not inside any of the deformed ellipsoids.

D. Truncation Stage: The Final 3-D Shapes

At the termination of the deformation stage, we truncate the deformed ellipsoids ($\mathcal{E}_{def}$) along their surfaces of intersection with the neighboring deformed ellipsoids and the resulting truncated ellipsoids represent the final 3-D reconstruction of the cells (Figure 3(B, C)). As an example, if $\mathcal{E}_{def}^{(k)}$ intersects with $\mathcal{E}_{def}^{(j_1)}$, $\mathcal{E}_{def}^{(j_2)} \cdots \mathcal{E}_{def}^{(j_\mathcal{N})}$, the 3-D reconstructed k^{th} cell is represented by

$$\text{Trunc}\left[\mathcal{E}_{def}^{(k)},\ \{\cup_{i=1}^{\mathcal{N}} \mathcal{E}_{def}^{(j_i)}\}\right] \tag{6}$$

where Trunc(A, B) represents the resultant shape of a solid body A when it is truncated by another solid body B and the 3D points ($p_c^{(k,j_i)}$) on the surface of of intersection of $\mathcal{E}_{def}^{(k)}$ and $\mathcal{E}_{def}^{(j_i)}$ satisfy the following,

$$\begin{aligned}&(p_c^{(k,j_i)} - c^{(k)})^T \Sigma^{(k)} (p_c^{(k,j_i)} - c^{(k)}) \\ &= (p_c^{(k,j_i)} - c^{(j_i)})^T \Sigma^{(j_i)} (p_c^{(k,j_i)} - c^{(j_i)})\end{aligned} \tag{7}$$

where $\mathcal{E}_{def}^{(k)}$ is the deformed ellipsoid with parameters $(c^{(k)}, \Sigma^{(k)})$ and $\mathcal{E}_{def}^{(j_i)}$ is the ellipsoid with parameters $(c^{(j_i)}, \Sigma^{(j_i)})$. The points $p_c^{(k)}$ inside the cell k must satisfy the following conditions

$$\begin{aligned}&(p_c^{(k)} - c^{(k)})^T \Sigma^{(k)} (p_c^{(k)} - c^{(k)}) \\ &< (p_c^{(k)} - c^{(j_i)})^T \Sigma^{(j_i)} (p_c^{(k)} - c^{(j_i)}) \quad \forall i \in \{1, \cdots \mathcal{N}\} \\ &\text{and } p_c^{(k)} \text{ must lie within } S^{SAM}\end{aligned} \tag{8}$$

The last condition, in fact, ensures that the cell k is bounded by the SAM surface if it is a peripheral cell. For visualization purpose, each cell can be represented by a polytope fitted to the surface points of the cell (Fig. 3(B, C)).

IV. Experimental Results

We have tested the proposed approach on a collection of around two hundred cells spanning multiple layers (e.g. L1, L2) in shoot apical meristem (SAM) of Arabidopsis Thaliana. The details of the generation of raw image data using CLSM technique, cell segmentation (we used Watershed segmentation [13] for all the experimental results shown) and cell tracking are described in Section II-A. The proposed 3D reconstruction scheme uses the preprocessed data for individual cells to estimate cell shapes in the cluster.

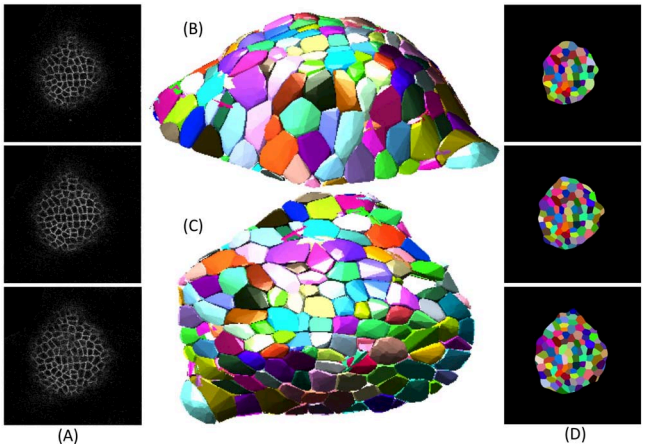

Figure 3. 3D Reconstruction of SAM Cell Cluster. (A) The original image slices at 1.5, 3, 4.5 μm depths in a 3D image stack, (B) The 3D reconstructed structure of a cluster of around 200 closely packed cells (a side view), (C) The same 3D structure viewed from top. The 3D structure can be computationally resliced along any arbitrary plane to obtain cross sectional slices, (D) The estimated cell walls when the 3D reconstruction is resliced with horizontal planes $z = 1.5, 3, 4.5\mu$m. While comparing to the actual cell walls, The computationally generated edges replicate the actual cell walls for majority of the cells.

A. Reconstruction of a Cluster of SAM Cells

After the necessary image preprocessing, segmentation and tracking to obtain correspondences between multiple slices of a cell in consecutive SAM layers (Fig. 3(A)), we ran our method to reconstruct the clusters as a collection of truncated ellipsoids representing the individual cells. The reconstructed 3D structure (Fig. 3(B): Viewed from a side, 3(C): Top view) closely resembles to the multilayered structure of the Arabidopsis SAM.

B. Validation of The Reconstruction Technique

There are no biological experiments which can directly validate the estimated growth statistics for individual cells in a multi layered cluster. In fact, the absence of a method to estimate growth statistics directly using non-computational methods in a live-imaging developmental biology framework is the motivation for the proposed work and we needed to design a method for computationally validating our 3D reconstruction technique. Once the 3D reconstruction is achieved, we can computationally reslice the reconstructed shape along any arbitrary viewing plane by simply collecting the subset of reconstructed 3D point cloud that lies on the plane. By choosing the reslicing plane as $z = 1.5, 3, 4.5\mu$m, we can computationally regenerate the cell walls for the previously chosen imaging planes along Z (Fig. 3(D)). The shapes of cells in the reconstructed slices can be compared against their counterparts in the raw images. The segmented cell slices are identical to the original image slices except for a number of cells in the periphery. The deviation in the reconstructed SAM slice boundary from the actual

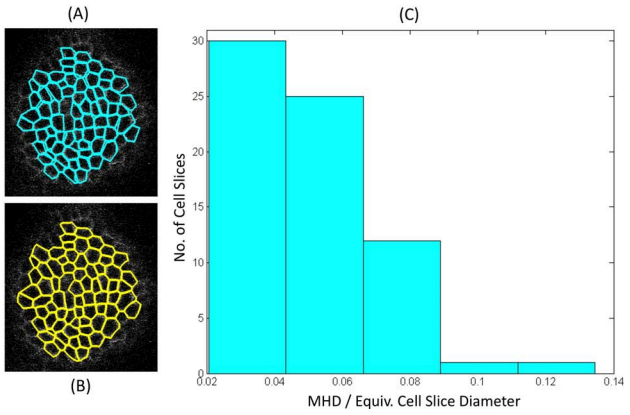

Figure 4. Validation of The 3D Reconstruction Method. (A) SAM image slice with the cell walls manually identified for 69 cells, (B) The same image slice with the computationally reconstructed cell walls, (C) Histogram of Modified Hausdorff Distances between each pair of individual cell shapes in original and reconstructed cell slices. The MHD for a cell is expressed as a fraction of the equivalent diameter of that cell in the slice to normalize the distance metric for various cell sizes.

image slices is the main source of error along with minor preprocessing errors on noisy images.

To quantify the accuracy of the reconstruction, for each pair of original and reconstructed slices of individual cells we compute Modified Hausdorff Distance (MHD) expressed as a fraction of the equivalent diameter of the original cell slice. This distance is an indicator of the error in reconstruction (analogous to the reprojection error widely used in the 3D reconstruction community to quantify the accuracy of reconstruction). Figure 4(A) shows a number of the cell walls manually marked on the raw image and Figure 4(B) presents the reconstructed cell walls for its corresponding reconstructed slice. The computed normalized MHDs for the cells are plotted in a histogram (Fig. 4(C)). For the majority of the cells the distance is very small (2 - 8 percent of the equivalent cell diameters). As mentioned earlier, the error in reconstruction is a little larger for a few cells at the SAM boundary. The SAM surface fitting strategy, described in Section III-B, imposes a smoothing constraint on the surface curvature and as a result the truncated cell edges for some cells in the periphery slightly deviates from the actual cell walls, seen in the confocal image slices.

V. Conclusion and Future Work

In this paper we have described a novel technique for 3D reconstruction at cell resolution of densely packed plant meristem cells from a very limited number of parallel cross sectional slices obtained through CLSM based live imaging technique. We proposed a multi-stage framework based on a deformed ellipsoidal approximation for individual cells and showed how we can reconstruct a cell cluster as a packing of truncated ellipsoids representing the individual cells. We tested this method on SAM cells of *Arabidopsis Thaliana* and obtained results which were validated computationally. As a direct application of this 3D reconstruction method, individual cell growth statistics such as cell volumes as a function of time can be obtained. Future work will involve computation of various cell growth statistics and detailed statistical analysis of the growth process based on the results obtained.

References

[1] T. Chan and L. Vese. Active contours without edges. *IEEE Trans. Image Process.*, 10:266–277, 2001.

[2] J. DErrico. Surface fitting using gridfit. In *MATLAB Central File Exchange*, 2005.

[3] R. J. Errington, M. D. Fricker, J. L. Wood, A. C. Hall, and N. S. White. Four-dimensional imaging of living chondrocytes in cartilage using confocal microscopy: a pragmatic approach. *Am. J. Physiol.*, 272(3):C1040–1051, 1997.

[4] J. Farinas, M. Kneen, M. Moore, and A. Verkman. Plasma membrane water permeability of cultured cells and epithelia measured by light microscopy with spatial filtering. *J. Gen. Physiol.*, 110(3):283–296, 1997.

[5] R. Fernandez, P. Das, V. Mirabet, E. Moscardi, J. Traas, J.-L. Verdeil, G. Malandain, and C. Godin. Imaging plant growth in 4d: robust tissue reconstruction and lineaging at cell resolution. *Nat Meth*, 7(7):547–553, 07 2010.

[6] E. Gor, V., T. M., Bacarian, and E. Mjolsness. Tracking cell signals in fluorescent images. *IEEE Workshop on Computer Vision Methods for Bioinformatics*, pages 142–150.

[7] K. Kawahara, M. Onodera, and Y. Fukuda. A simple method for continuous measurement of cell height during a volume change in a single a6 cell. *Jpn. J. Physiol*, pages 411–419, 1994.

[8] L. G. Khachiyan. Rounding of polytopes in the real number model of computation. *Math. Oper. Res.*, pages 307–320, 1996.

[9] P. Kumar and E. A. Yildirim. Minimum-volume enclosing ellipsoids and core sets. *Journal of Optimization Theory and Applications*, 126:1–21, 2005.

[10] M. Liu, R. K. Yadav, A. Roy-Chowdhury, and G. V. Reddy. Automated tracking of stem cell lineages of arabidopsis shoot apex using local graph matching. *Plant journal, Oxford, UK*, 62:135–147, 2010.

[11] H. Mebatsion, P. Verboven, A. Melese Endalew, J. Billen, Q. Ho, and B. Nicola. A novel method for 3-d microstructure modeling of pome fruit tissue using synchrotron radiation tomography images. *Journal of Food Engineering*, 93:141–148, 2009.

[12] T. Nakahari, M. Murakami, H. Yoshida, M. Miyamoto, Y. Sohma, and Y. Imai. Decrease in rat submandibular acinar cell volume during ach stimulation. *Am. J. Physiol.*, 258(6):G878–886, 1990.

[13] L. Vincent and P. Soille. Watersheds in digital spaces: An efficient algorithm based on immersion simulations. *IEEE Transactions on Pattern Analysis and Machine Intelligence, 1991*, 13(6):583–598, 1991.

[14] P. Viola and W. M. Wells. Alignment by maximization of mutual information. *International Journal of Computer Vision*, 24(2):137–154, 1997.

[15] J. Wyrzykowska and A. Fleming. Cell division pattern influences gene expression in the shoot apical meristem. *PNAS*, 100(9):5561–5566, 2003.

[16] Z. Yin, R. Bise, M. Chen, and T. Kanade. Cell segmentation in microscopy imagery using a bag of local bayesian classifiers. In *Proceedings of the 2010 IEEE international conference on Biomedical imaging: from nano to Macro*, pages 125–128, 2010.